ACCOUNTS of chemical research

Article

pubs.acs.org/accounts

Diverse Photoinduced Dynamics in an Organic Charge-Transfer Complex Having Strong Electron−Phonon Interactions

Ken Onda,*[,†,‡] Hideki Yamochi,[§] and Shin-ya Koshihara[∥,⊥]

[†]Interactive Research Center of Science, Tokyo Institute of Technology, Nagatsuta, Midori-ku, Yokohama, Kanagawa 226-8502, Japan
[‡]PRESTO, Japan Science and Technology Agency (JST), 4-1-8 Honcho, Kawaguchi, Saitama 332-0012, Japan
[§]Research Center for Low Temperature and Materials Sciences, Kyoto University, Sakyo-ku, Kyoto 606-8501, Japan
[∥]Department of Chemistry and Materials Science, Tokyo Institute of Technology, O-okayama, Meguro-ku, Tokyo 152-8551, Japan
[⊥]CREST, Japan Science and Technology Agency (JST), O-okayama, Meguro-ku, Tokyo 152-8551, Japan

CONSPECTUS: Phenomena that occur in nonequilibrium states created by photoexcitation differ qualitatively from those that occur at thermal equilibrium, and various physical theories developed for thermal equilibrium states can hardly be applied to such phenomena. Recently it has been realized that understanding phenomena in nonequilibrium states in solids is important for photoenergy usage and ultrafast computing. Consequently, much effort has been devoted to revealing such phenomena by developing various ultrafast observation techniques and theories applicable to nonequilibrium states. This Account describes our recent studies of diverse photoinduced dynamics in a strongly correlated organic solid using various ultrafast techniques. Solids in which the electronic behavior is affected by Coulomb interactions between electrons are designated as strongly correlated materials and are known to exhibit unique physical properties even at thermal equilibrium. Among them, many organic charge-transfer (CT) complexes have low dimensionality and flexibility in addition to strong correlations; thus, their physical properties change sensitively in response to changes in pressure or electric field. Photoexcitation is also expected to drastically change their physical properties and would be useful for ultrafast photoswitching devices. However, in nonequilibrium states, the complicated dynamics due to these characteristics prevents us from understanding and using these materials for photonic devices.

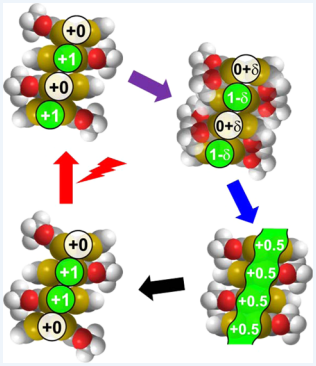

The CT complex $(EDO\text{-}TTF)_2PF_6$ (EDO-TTF = 4,5-ethylenedioxytetrathiafulvalene) exhibits unique photoinduced dynamics due to strong electron−electron and electron−phonon interactions. We have performed detailed studies of the dynamics of this complex using transient electronic spectroscopy at the 10 and 100 fs time scales. These studies include transient vibrational spectroscopy, which is sensitive to the charges and structures of constituent molecules, and transient electron diffraction, which provides direct information on the crystal structure. Photoexcitation of the charge-ordered low-temperature phase of $(EDO\text{-}TTF)_2PF_6$ creates a new photoinduced phase over 40 fs via the Franck−Condon state, in which electrons and vibrations are coherently and strongly coupled. This new photoinduced phase is assigned to an insulator-like state in which the charge order differs from that of the initial state. In the photoinduced phase, translations of component molecules proceed before the rearrangements of intramolecular conformations. Subsequently, the charge order and structure gradually approach those of the high-temperature phase over 100 ps. This unusual two-step photoinduced phase transition presumably originates from steric effects due to the bent EDO-TTF as well as strong electron−lattice interactions.

1. INTRODUCTION

Charge-transfer (CT) complexes are molecular crystals that consist of both an electron donor and an electron acceptor.[1−4] When electron transfer occurs between the donor and acceptor, provided that the degree of electron transfer and the crystal structures are appropriate at thermal equilibrium, CT complexes have an unfilled band and acquire metallic or semiconductor-like characteristics. Such electrically conducting CT complexes include small π-conjugated molecules, and when planar molecules are present, the band structure is one- or two-dimensional because of the anisotropy of π orbitals. Because overlap between the π orbitals (as measured by the transfer integral, t) is small ($t \sim 0.1$ eV) compared with typical inorganic metals, CT complexes are strongly correlated materials. These crystals are soft and flexible as a result of the weak interactions between molecules. In addition, the molecular structure itself is often strongly coupled with the degree of CT. The low dimensionality, strong electron correlations, and flexibility lead to diverse physical properties, and their pressure−temperature phase diagrams are complicated. These characteristics make CT complexes very sensitive to changes in their environment, such as changes in pressure, temperature, and electric field.

Despite their complicated crystal structures, the electronic states of CT complexes can be understood using a simple

Received: July 23, 2014
Published: October 23, 2014

   dx.doi.org/10.1021/ar500257b | Acc. Chem. Res. 2014, 47, 3494−3503

model based on the tight-binding model, which assumes ordered ion cores and electrons bound by the cores.[5−7] For the constituent π-conjugated molecules of a CT complex, only the frontier orbitals are considered to be electronic orbitals, and the rest are regarded as the ionic core. Because the crystal structure can be determined by X-ray crystal structure analysis, transfer integrals between constituent molecules are easily calculated.[5,6] For electron correlations, an effective model is the extended Hubbard model,[7] in which the Hamiltonian includes on-site Coulomb interactions (U) and nearest-neighbor Coulomb interactions (V). Terms for electron−phonon interactions can also be included in this Hamiltonian, as described below. Thus, the electronic states of CT complexes are easily treated theoretically, although they are complicated molecular solids.

Not only do CT complexes have controllable physical properties and easy-to-understand electronic states, but also their crystal structures can be designed using organic synthesis. Thus, they are ideal models for understanding the fundamental physics of solid materials. These characteristics are also suitable for photocontrol of the physical properties of solid materials, so the photoinduced dynamics of CT complexes has been studied intensively. For example, a photoinduced phase transition (PIPT) was first discovered[8−11] for the CT complex tetrathiafulvalene-*p*-chloranil (TTF-CA), which undergoes a neutral-to-ionic phase transition. Tetracyanoquinodimethane (TCNQ) salts with alkali metals having one-dimensional half-filled electronic systems exhibit a typical PIPT based on their one dimensional nature.[12,13] The salt bis(ethylenedithio)-tetrathiafulvalene (BEDT-TTF) is well-known to form CT complexes having two-dimensional electronic systems and to show various types of PIPTs depending on the crystal structure.[14,15] The salt $Pd(dmit)_2$ (dmit = 1,3-dithiole-2-thione-4,5-dithiolate) forms strongly bound dimers in the complexes and exhibits a PIPT relevant to dimerization.[16,17] The CT complex $(EDO\text{-}TTF)_2PF_6$ (EDO-TTF = 4,5-ethylenedioxytetrathiafulvalene) is a quasi-one-dimensional three-fourths-filled electronic system and has strong electron−phonon interactions in addition to electron−electron interactions.[18,19] In this Account, we describe the diverse photoinduced dynamics of $(EDO\text{-}TTF)_2PF_6$ originating from the strong electron−phonon interactions.

2. OPTICAL SPECTRA OF $(EDO\text{-}TTF)_2PF_6$

At room temperature, $(EDO\text{-}TTF)_2PF_6$ is a quasi-one-dimensional organic conductor and a black shiny crystal, as shown in Figure 1a.[20−24] The molecular structure of the donor EDO-TTF molecule is shown in Figure 1b. Figure 1c shows the crystal structure of this complex at room temperature; a quasi-one-dimensional band along the stacking direction of EDO-TTF is formed in the crystal by overlapping π orbitals of EDO-TTF. The band becomes three-fourths-filled by transfer of one electron from every two EDO-TTF molecules to a PF_6 molecule. Because of the Peierls instability, one-dimensional electronic structures tend to be insulators. In addition, the electronic structure of the complex is affected by charge and anion order due to electron−electron and electron−phonon interactions. Consequently, charge is localized at each EDO-TTF, and the complex becomes an insulator below T_c = 280 K. The crystal structure of this insulator phase is shown in Figure 1d. From infrared and Raman spectroscopies and X-ray structural analyses, the charge order is determined to be ···, 0, 1, 1, 0, ···, which we hereafter abbreviate as (0, 1, 1, 0). One unique feature of this material is that the molecular shape of

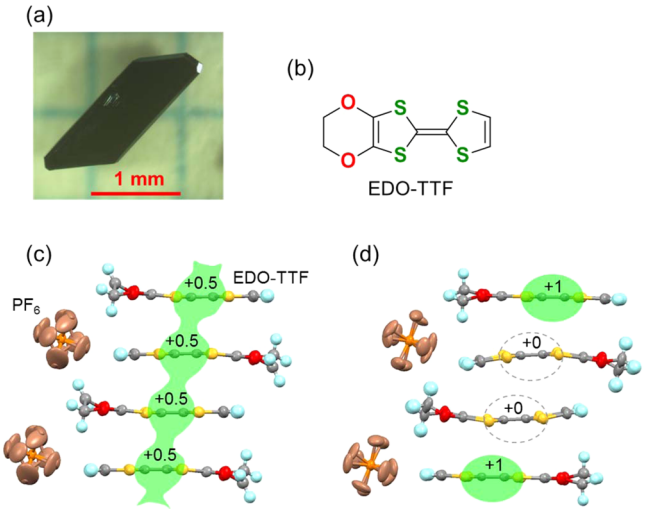

Figure 1. (a) Single crystal of $(EDO\text{-}TTF)_2PF_6$. (b) Chemical structure of EDO-TTF. (c, d) Crystal structures in the (c) high-temperature and (d) low-temperature phases.

EDO-TTF is strongly affected by its charge: EDO-TTFs with charges of 0, +1, and +0.5 have bent, flat, and nearly flat shapes, respectively. This indicates that this material has strong interactions between electrons and intramolecular vibrations as well as intermolecular interactions.

Figure 2 shows (a) reflectivity and (b) optical conductivity spectra of $(EDO\text{-}TTF)_2PF_6$ in the low- and high-temperature phases. The optical conductivity spectra were obtained from the reflectivity spectra by the Kramers−Kronig (K−K) transformation. In the high-temperature phase at 290 K, there is a Drude-like reflectivity increase below 0.8 eV. In contrast, in the low-temperature phase at 180 K, the optical conductivity approaches zero at low photon energies, and there are two CT bands, one at 0.6 eV (CT1), and the other at 1.4 eV (CT2). Another CT band (CT3) is located at the shoulder of CT1 on the higher photon energy side; CT3 is more clearly seen in the spectrum at 10 K. On the basis of a simple model calculation for the (0, 1, 1, 0) charge localization, CT1 is assigned to the transition between neutral and monovalent EDO-TTF molecules, CT2 to the transition between adjacent monovalent EDO-TTF molecules, and CT3 to a mixture of these two transitions.[24]

3. EMERGENCE OF A PHOTOINDUCED PHASE AND ITS QUANTUM COHERENCE

In solids, the initial process of photoinduced dynamics is extremely fast because of the high density of electronic states. To study such a fast process, we generated a 12 fs pulse from a conventional Ti:sapphire amplifier and located the photon energy of the pulse in the vicinity of the CT2 band; we measured changes in transient reflectivity using this pulse for both the pump and probe pulses.[25] Figure 3a shows temporal changes in reflectivity at around 1.65 eV after the photoexcitation of the CT2 transition in the low-temperature phase at 25 K. This temporal profile has three characteristic features: (1) a fast rise at around zero delay, (2) a slow rise following the fast rise, and (3) weak oscillations in the region of negative delay. The fast and slow rises are explained by the simple three-level model shown in Figure 3b. The system is excited from the ground state to the Franck−Condon state (the CT2 state) by a pulse expressed as a Gaussian function ($G(t)$). Subsequently,

dx.doi.org/10.1021/ar500257b | Acc. Chem. Res. 2014, 47, 3494−3503

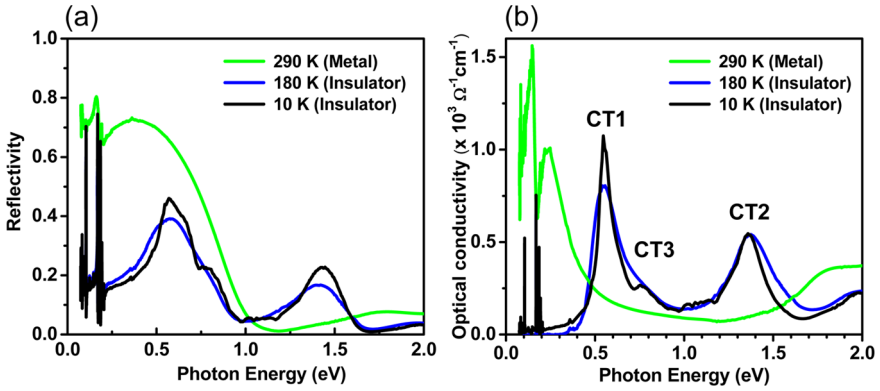

Figure 2. (a) Reflectivity and (b) optical conductivity spectra of $(EDO\text{-}TTF)_2PF_6$ at 290 K in the metallic high-temperature phase (green) and in the insulating low-temperature phase at 180 K (blue) and 10 K (black).

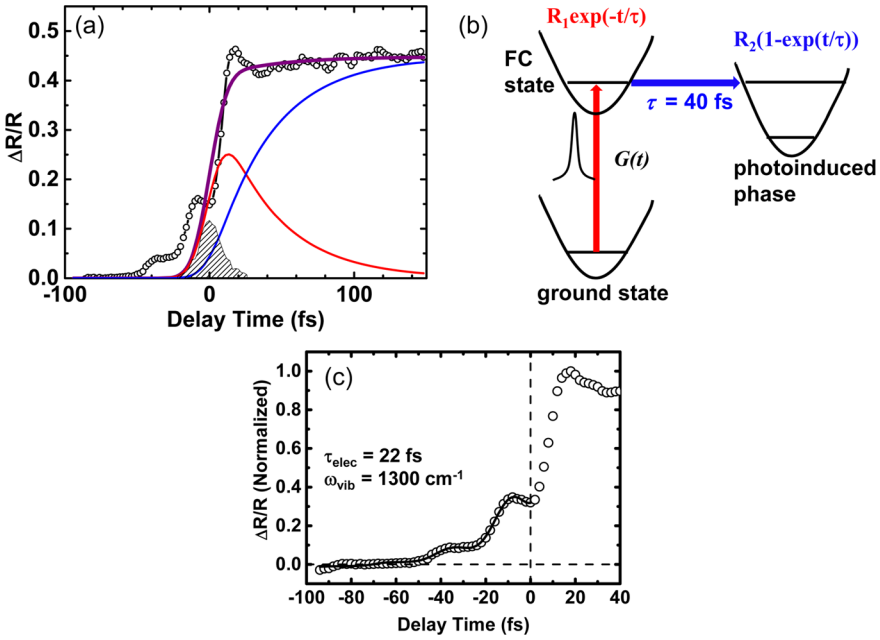

Figure 3. (a) Experimental (circles) and simulated (solid lines) temporal profiles of reflectivity changes after photoexcitation at 1.65 eV in $(EDO\text{-}TTF)_2PF_6$ at 25 K. The hatched area is the autocorrelation of the pump and probe pulses. (b) Model of the initial process used in the simulation. (c) Enlarged view of the temporal profile in the negative delay region (circles). The solid line is a fit to an exponential function and a damped oscillation.

the CT2 state exponentially changes to another state with time constant τ. Using this model, we fit the data, including more data not shown here, and obtained the time constant τ = 40 fs, indicating that it takes 40 fs for the new state to emerge. This emerging state is assigned to the photoinduced state, which is observed only by photoexcitation, as described in section 4.

A negative delay signal is known to appear as a result of third-order nonlinear optical processes,[26−28] and it can be used to obtain information on the electronic and vibrational coherence in the directly excited state, the CT2 state in this case.[29] By fitting the data using an exponential function and a damped oscillation, as shown in Figure 3c, we obtained the time constant τ_{elec} = 22 fs for the decay time of electronic coherence and ω_{vib} = 1300 cm^{-1} for the wavenumber of the coherent vibrations. This wavenumber is close to those of C═C stretching vibrations of EDO-TTF in the Raman spectrum at 1400−1700 cm^{-1};[24] thus, the 1300 cm^{-1} oscillation is assignable to the intramolecular vibrations of EDO-TTF. The slight softening from the Raman peaks is presumably attributed to modulation of the vibration in the excited state by the CT transition. Because the photoinduced state emerges immediately after the disappearance of this electronic and vibrational coherence, we conclude that strong electron−vibration coupling plays an important role in the emergence of the photoinduced state. Similar strong coupling between the CT and C═C vibrations associated with the PIPT have also been observed in the BEDT-TTF system.[30]

4. CHARACTERISTICS OF THE PHOTOINDUCED PHASE

The reflectivity change of about 50% shown in Figure 3a is anomalously large compared with those in conventional materials. Even larger changes of more than 100% were observed at another probe photon energy from measurements using a 100 fs pulse.[18] This indicates that the photoinduced state has a largely different character from the low-temperature phase. We also determined that the change in reflectivity increases nonlinearly as the excitation pulse energy increases, and the increase begins at a certain energy, that is, it has a threshold.[18] This means that the photoinduced state emerges

dx.doi.org/10.1021/ar500257b | Acc. Chem. Res. 2014, 47, 3494−3503

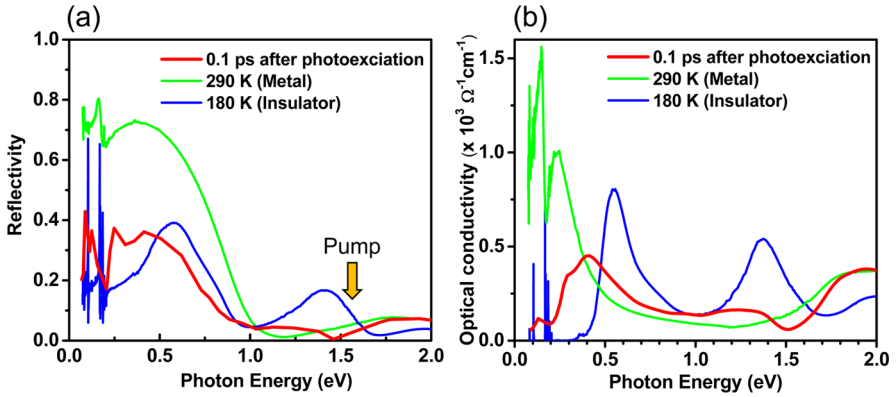

Figure 4. (a) Transient reflectivity and (b) optical conductivity spectra at 0.1 ps after the photoexcitation of $(EDO\text{-}TTF)_2PF_6$ in the low-temperature phase at 180 K (red). For comparison, static spectra at 290 K (green) and 180 K (blue).

cooperatively. The efficiency of creation of the photoinduced state was estimated by assuming that the high-temperature phase is created by photoexcitation (this assumption is incorrect, as described below), and the obtained values were much larger than unity. These results indicate that one photon changes many molecules cooperatively. This phenomenon is called a PIPT, although the photoinduced phase is not exactly the same as a phase occurring at thermal equilibrium.[31,32]

To learn more details about the photoinduced phase, reflectivity spectra over a wide range of photon energies are needed to allow comparisons with those in thermal equilibrium, which were interpreted in section 2. In Figure 4a, the red line is the transient reflectivity spectrum 0.1 ps after photoexcitation of the low-temperature phase at 180 K.[19,33] The temporal width and photon energy of the excitation pulse were 120 fs and 1.55 eV, respectively. This spectrum was constructed from the sum of the reflectivity change ($\Delta R/R$) spectrum after photoexcitation and the reflectivity (R) spectrum before photoexcitation. For comparison, the reflectivity spectra in the high-temperature (green line) and low-temperature (blue line) phases are also shown in Figure 4a. Figure 4b shows the optical conductivity spectra obtained from the reflectivity spectra by the K−K transformation with appropriate extrapolations.

Figure 4 shows that the transient spectra after photoexcitation differ from those at thermal equilibrium, indicating that the photoinduced phase cannot be assigned to either the low- or high-temperature phase. In other words, we detected a state created only by photoexcitation or a hidden state. The reflectivity and optical conductivity approach zero as the photon energy decreases, and only one band, probably arising from the CT transition, is located at 0.4 eV, indicating that the photoinduced phase is insulator-like and has a different charge distribution from the (0, 1, 1, 0) distribution of the low-temperature phase.

To assign this photoinduced original phase, we performed a model calculation based on the extended Hubbard model. To include electron−phonon interactions in this model, we introduced Peierls-type (modulation of transfer integrals) and Holstein-type (modulation of site energies) electron−phonon couplings.[19,34] The total Hamiltonian was

$$
\begin{aligned}
H = &-\sum_{j,\sigma}[t_0 - \alpha(u_{j+1} - u_j)](c_{j,\sigma}^{\dagger}c_{j+1,\sigma} + \text{h.c.}) \\
&- \beta\sum_j v_j\left(n_j - \frac{1}{2}\right) + U\sum_j n_{j,\uparrow}n_{j,\downarrow} \\
&+ \frac{1}{2}K_\alpha\sum_j (u_{j+1} - u_j)^2 + \frac{1}{2}K_\beta\sum_j v_j^2 + \frac{2K_\alpha}{\omega_\alpha^2}\sum_j \dot{u}_j^2 \\
&+ \frac{K_\beta}{2\omega_\beta^2}\sum_j \dot{v}_j^2 - \gamma\sum_l w_l(n_{2l-1} + n_{2l} - 1) \\
&+ \frac{1}{2}K_\gamma\sum_l w_l^2 + \frac{K_\gamma}{2\omega_\gamma^2}\sum_l \dot{w}_l^2 + V\sum_j n_j n_{j+1}
\end{aligned}
\tag{1}
$$

As shown schematically in Figure 5a, t_0 represents the bare transfer integral, while U and V are the on-site and nearest-neighbor Coulomb interactions, respectively. Electron−phonon interactions are shown schematically in Figure 5b. The parameters α, β, and γ are the electron−phonon coupling strengths that modulate the transfer integrals by molecular displacements, the site energies by molecular deformations, and the site energies by anion displacements, respectively. In eq 1, K_α, K_β, and K_γ are the corresponding spring constants, whereas ω_α, ω_β, and ω_γ are the corresponding bare phonon frequencies. These parameters were determined when the calculated

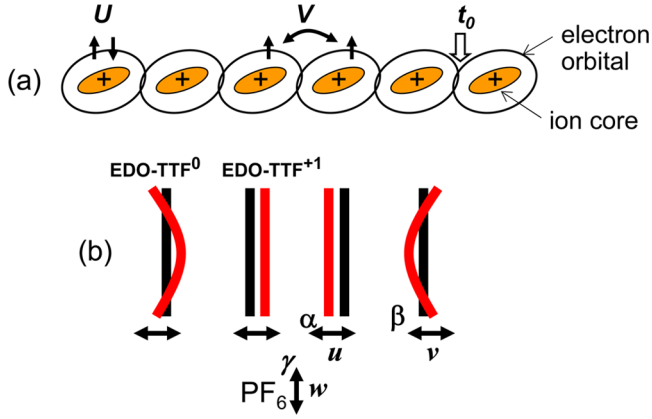

Figure 5. Schematic illustration of the interaction parameters used in eq 1 for model calculations. (a) U is the on-site Coulomb interaction, V is the nearest-neighbor Coulomb interaction, and t_0 is the bare transfer integral. (b) The parameters α, β, and γ are electron−phonon coupling strengths.

dx.doi.org/10.1021/ar500257b | Acc. Chem. Res. 2014, 47, 3494−3503

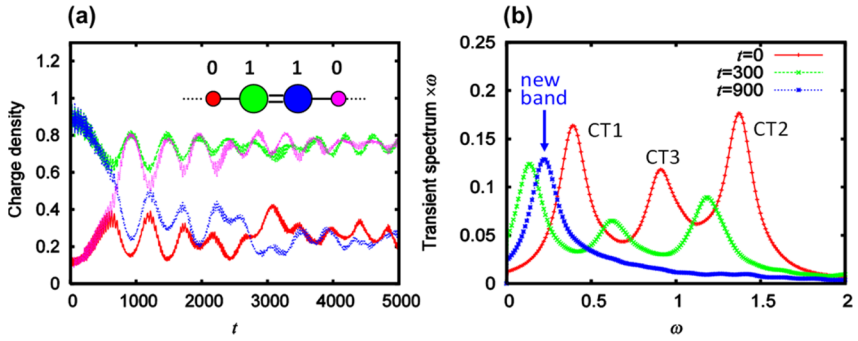

Figure 6. (a) Temporal variations of the charge on each EDO-TTF molecule obtained from the model calculation. Colors correspond to EDO-TTF sites, and t is the temporal parameter for the calculation. (b) Calculated transient spectra at t = 0, 300, and 900.

spectrum was close to the observed one in the low-temperature phase. Photoexcitation was introduced as a time-dependent electric field, and the temporal evolution of the system was calculated by solving the time-dependent Schrödinger equation.[19]

Figure 6 summarizes the results of the calculation. Figure 6a shows the temporal variations of the charge on each EDO-TTF molecule. The horizontal axis (t) does not directly correspond to the experimental delay time; t = 1520 roughly corresponds to 1 ps. The results show that after the electric field was applied from t = 0 to 209 as an excitation pulse, the charge distribution suddenly changed at t = 700. At this time, the charge order (0, 1, 1, 0) changed to approximately (0, 1, 0, 1). Figure 6b shows the variations in the calculated spectra at t = 0, 300, and 900. At t = 0, the spectrum has three bands corresponding to the three CT transitions in the low-temperature phase. At t = 900, only one band appears and is assigned to the CT transition between neutral and monovalent EDO-TTFs in the (0, 1, 0, 1) charge order. This calculated result is in good agreement with the experimental one, that is, another state emerges some time after photoexcitation, and the three CT bands change to one CT band. Thus, we assigned the photoinduced phase that emerges after 40 fs to the (0, 1, 0, 1) charge-ordered state. However, it should be noted that the range of this charge order is not very long, and both the charge distribution and structure fluctuate in this phase.

5. FOLLOWING PROCESS AND THE MELTING OF CHARGE ORDER

As described so far, the state at around 100 fs after photoexcitation has never been observed at thermal equilibrium. After this state forms and a sufficient time has elapsed, the system must revert to the low-temperature phase. What happens during this time? Figure 7 shows temporal profiles for reflectivity changes up to 1000 ps at selected probe photon energies.[33,35] After the quick reflectivity increase/decrease, which corresponds to the emergence of the photoinduced phase, the reflectivity change decreases/increases with oscillations having a period of 0.5 ps; this corresponds to 66 cm^{-1}. Judging from this wavenumber, the coherent oscillations are attributed to intermolecular vibrations between EDO-TTF molecules. This indicates that intermolecular vibrations are involved in the relaxation from the photoinduced state. Even after 3 ps, reflectivity changes persist and their signs are inverted, indicating that a new state emerges in this time region although most parts relax to the initial state. The irregular oscillations above 500 ps that accompany these reflectivity changes are attributed to a shock wave traveling inside the

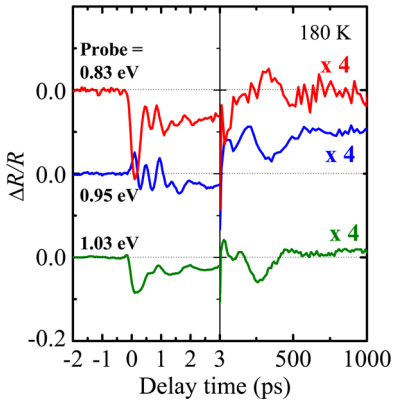

Figure 7. Temporal profiles of reflectivity changes ($\Delta R/R$) in the near-infrared region at 0.83 (red), 0.95 (blue), and 1.03 (dark green) eV upon photoexcitation at 1.55 eV in the insulating low-temperature phase of $(EDO\text{-}TTF)_2PF_6$ at 180 K. Adapted from ref 35. Copyright 2012 American Chemical Society.

crystal. However, it is difficult to identify the long-lived state from the electronic spectral changes derived from these reflectivity changes; thus, we need another method that is sensitive to charge and structural changes of molecules.

One such method is time-resolved vibrational spectroscopy. In general, organic molecules have many vibrational transitions in the mid-infrared region, and the energies and intensities of these transitions are sensitive to the charge and structure of the molecule. Measurement of such vibrational spectra on a picosecond time scale thus becomes a powerful tool for real-time observations of charge and structural changes of molecules even in an organic crystal. We constructed such measurement systems that were specialized for the photoinduced dynamics of organic crystals.[17,35−37] Figure 8a shows transient reflectivity changes in the range from 1300 to 1700 cm^{-1} at 1, 20, and 300 ps after photoexcitation of the CT2 band in the low-temperature phase.[35] The energy and temporal width of the pulse for these measurements were 10 cm^{-1} and 3 ps, respectively. In this wavenumber region, there are vibrational peaks assigned to C═C stretching vibrations of π-conjugated molecules, such as EDO-TTF; these peaks are often used as indicators of charge and structural changes in various CT complexes.[24,38,39] The figure also contains reflectivity spectra in the high-temperature (green line) and low-temperature (blue line) phases at thermal equilibrium. The polarization of the infrared light was perpendicular to the direction of one-dimensional electric conduction; thus, no reflectivity increase

dx.doi.org/10.1021/ar500257b | Acc. Chem. Res. 2014, 47, 3494−3503

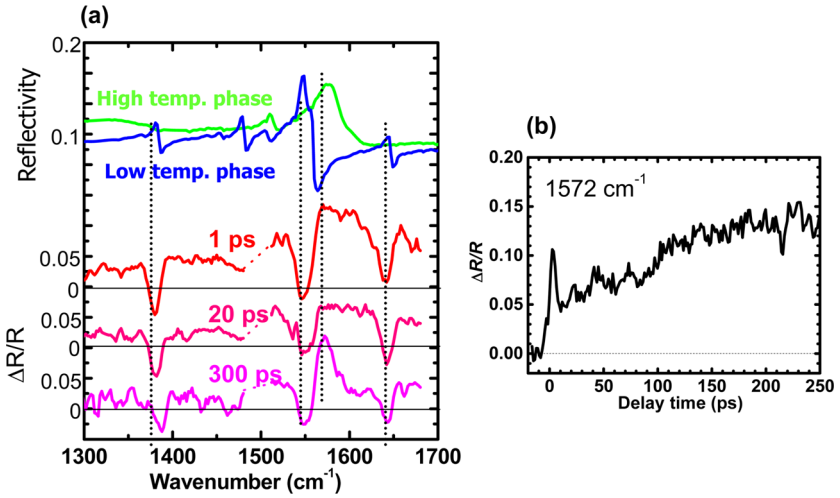

Figure 8. (a) Reflectivity change ($\Delta R/R$) spectra in the molecular vibration region at 1, 20, and 300 ps after photoexcitation of $(EDO\text{-}TTF)_2PF_6$ at 180 K (red) and static reflectivity (R) spectra of the high-temperature phase at 290 K (green) and the low-temperature phase at 180 K (blue). (b) Temporal profile of the reflectivity change ($\Delta R/R$) at 1572 cm^{-1}.

due to conduction electrons was observed, even in the high-temperature metallic phase.

In the transient spectrum at 1 ps after photoexcitation, the reflectivity sharply decreases at the positions of the peaks in the low-temperature phase, indicating that the low-temperature phase disappeared. Simultaneously, the reflectivity broadly increases over the observed range, indicating that some carriers emerge along the direction perpendicular to stacking direction and/or that the peaks are broadened as a result of charge and structural fluctuations. At 20 ps, the sharp reflectivity decreases remain, while the broad increase over the entire observed range decreases. Then at 300 ps a peak at 1572 cm^{-1} emerges. Because the wavenumber of the peak agrees with that of the peak in the high-temperature phase, the emergence of this peak indicates the emergence of a new state that is similar to the high-temperature phase. Figure 8b shows the temporal profile of the reflectivity change at this peak position. Immediately after photoexcitation, the reflectivity increases quickly and soon decreases; subsequently, it gradually increases again over ~100 ps. This temporal change means that 100 ps is required for the emergence of the high-temperature-like phase.

Figure 9 summarizes the photoinduced dynamics elucidated by time-resolved infrared vibrational spectroscopy and the other techniques described so far. Photoirradiation of the crystal in the low-temperature phase, in which the charge is localized and ordered as (0, 1, 1, 0), creates a photoinduced phase having a different charge order of (0, 1, 0, 1) after 40 fs. The fluctuating charge and the structure of the new state cause broad increases in reflectivity along the direction perpendicular to the conducting direction. After that, the band becomes broader as the fluctuations become larger, and the reflectivity in the observed region decreases. Eventually, the charge order is completely melted, and holes are distributed evenly along the conducting direction. Because this state has the same character as the high-temperature phase, a peak emerges at the same position as that for the high-temperature phase. It takes 100 ps for this process to occur.

In solids, relaxation from a photoexcited state is generally very quick because the state interacts with many electronic and vibrational states. Thus, the obtained time scale of 100 ps appears to be very long for a solid. However, we have found slow processes of over tens of picoseconds in other CT

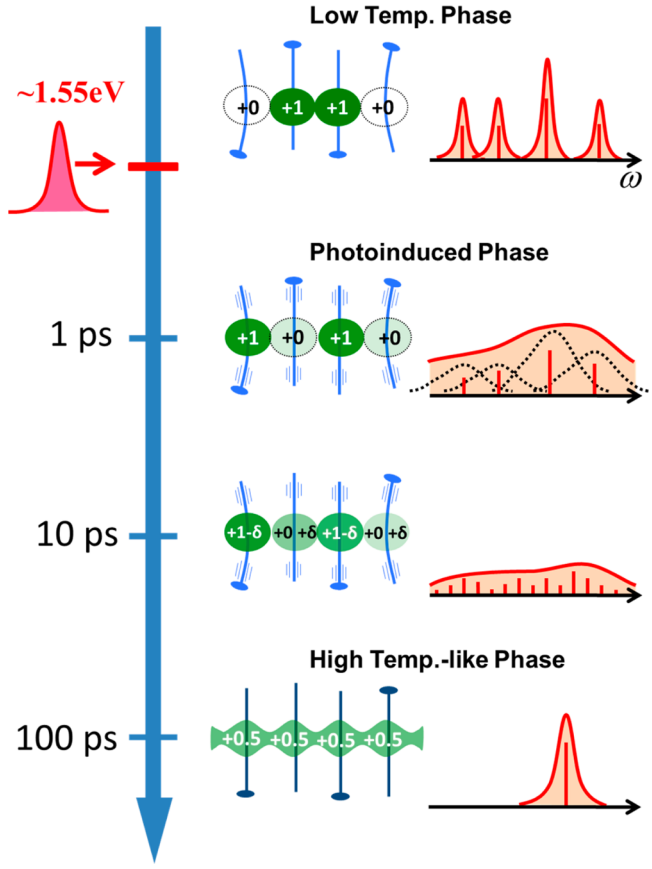

Figure 9. Schematic illustration of the proposed time evolution of the charge pattern and molecular structure after the photoexcitation of the charge-ordered insulating phase in $(EDO\text{-}TTF)_2PF_6$. The illustrations at the right show the spectra in the molecular vibrational region expected on the basis of these charge patterns and molecular structures. Adapted from ref 35. Copyright 2012 American Chemical Society.

complexes,[17,40] so we believe that this slow process can occur in some types of solids. What is the origin of this slow process? Although the detailed mechanism is unclear, in our previous studies slow processes were observed in crystals that experience

dx.doi.org/10.1021/ar500257b | Acc. Chem. Res. 2014, 47, 3494−3503

large steric hindrance during phase transitions.[17] Moreover, as described in section 6, some molecules vary slowly over ∼100 ps after photoexcitation while other molecules vary over less than 1 ps, even in a single crystal. It was found that slowly varying molecules undergo large deformations during phase transitions. Thus, relations between slow photoinduced structural changes and steric effects should be investigated further, both experimentally and theoretically.

6. DIRECT OBSERVATION OF STRUCTURAL CHANGES USING TIME-RESOLVED DIFFRACTION

So far we have reviewed photoinduced dynamics from the Franck−Condon state to the charge melting state in terms of optical spectroscopy. However, these optical spectroscopic methods can provide only indirect information on structural changes. To obtain the crystal order of atoms in real space (i.e., the crystal structure), diffraction methods using X-rays or electrons are generally used. If such a diffraction method can acquire temporal resolution on the order of femto- or picoseconds, it becomes possible to see crystal structure changes at every moment, that is, a movie of the molecular motion could be made. One such method is time-resolved electron diffraction using an ultrashort-pulse laser. An ultrashort electron bunch is generated by irradiation of a metal foil with an ultrashort pulse in which the photon energy of the pulse is a little higher than the work function of the metal. Thus, a 100 fs electron bunch can be obtained from a 100 fs optical pulse; however, such an electron bunch stretches soon after generation because of Coulomb repulsions between electrons. Recently, various techniques have been developed to overcome this difficulty.[40−44]

Figure 10 shows diffraction patterns of $(EDO\text{-}TTF)_2PF_6$ in the (left) low- and (right) high-temperature phases obtained by

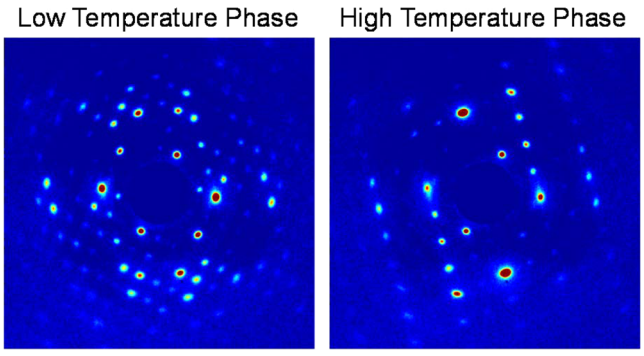

Figure 10. Diffraction patterns of $(EDO\text{-}TTF)_2PF_6$ in (left) the low-temperature phase at 230 K and (right) the high-temperature phase at 295 K.

using such an ultrashort electron bunch.[45] These diffraction patterns are in good agreement with simulated patterns based on the parameters obtained from a conventional X-ray diffraction. Figure 11a shows the temporal variations in the difference in the diffraction patterns before and after photoexcitation of the low-temperature phase. Figure 11b shows the temporal variations in the relative intensity change for selected diffraction spots. The variations for all of the spots increase immediately after photoexcitation, soon decrease, and subsequently increase again slowly over ∼100 ps. This temporal behavior is similar to that of the vibrational peak assigned to the metal-like phase as described in section 5. This means that the

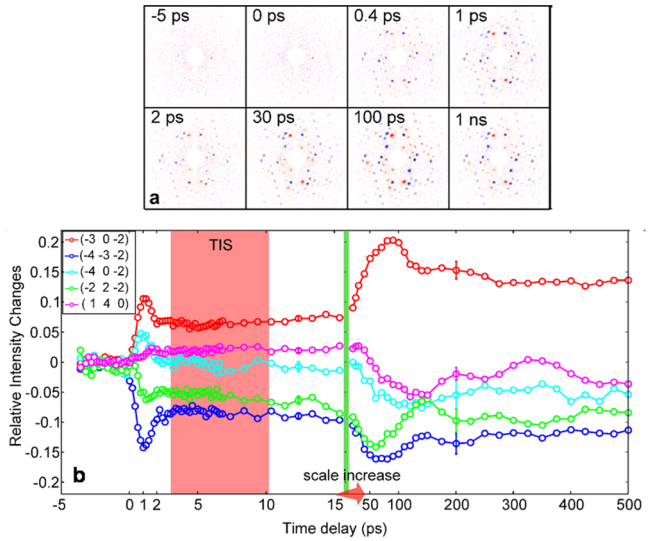

Figure 11. (a) Difference in diffraction patterns at each delay time before and after photoexcitation at time zero. (b) Temporal variations in the relative intensity changes for selected diffraction spots. Adapted with permission from ref 45. Copyright 2013 Nature Publishing Group.

data obtained from time-resolved diffraction and the data acquired using vibrational methods describe the same photoinduced dynamics in $(EDO\text{-}TTF)_2PF_6$.

Each time-delayed diffraction pattern contains hundreds of Bragg reflections; however, they are not enough to carry out a general structural refinement procedure. Therefore, we used a model refinement using a linear interpolation between the atomic positions in the low- and high-temperature phases and obtained nice convergence of the Pearson correlation coefficient across the complete time span.[45] To express the progression of the photoinduced phase transition, the modulations of atomic coordinates are grouped as ξ_F, ξ_B, and ξ_P to express the modulations of flat (+1 charged) and bent (neutral) EDO-TTF molecules and the PF_6 anion, respectively. The parameters ξ_F, ξ_B, and ξ_P are regarded as those of reaction coordinates corresponding mainly to the translation and flattening of each EDO-TTF and the motion of the PF_6 anion, respectively. Figure 12a shows the temporal variations of these three parameters, where the values (ξ_F, ξ_B, ξ_P) for the structures in the low- and high-temperature phases are set to (0, 0, 0) and (1, 1, 1), respectively. After photoexcitation, the structure quickly changes toward that in the high-temperature phase; however, the progression along ξ_B is much smaller than those along ξ_F and ξ_P. This indicates that the flattening of the bent neutral EDO-TTF is much slower than the motions of flat monovalent EDO-TTF and PF_6. Soon after this structural change, these displacements partially revert back to the structure in the low-temperature phase. Subsequently, the structure gradually changes again toward that in the high-temperature phase. Finally, after ∼100 ps, the structure becomes the same as that in the high-temperature phase. Figure 12b shows the crystal structural changes estimated from these measurements. The central cell shows the crystal structure in the low-temperature phase with the molecules represented by a capped stick model. The left and right cells show displacements from the structure in the low-temperature phase (green bars) for the transient intermediate structure

dx.doi.org/10.1021/ar500257b | Acc. Chem. Res. 2014, 47, 3494−3503

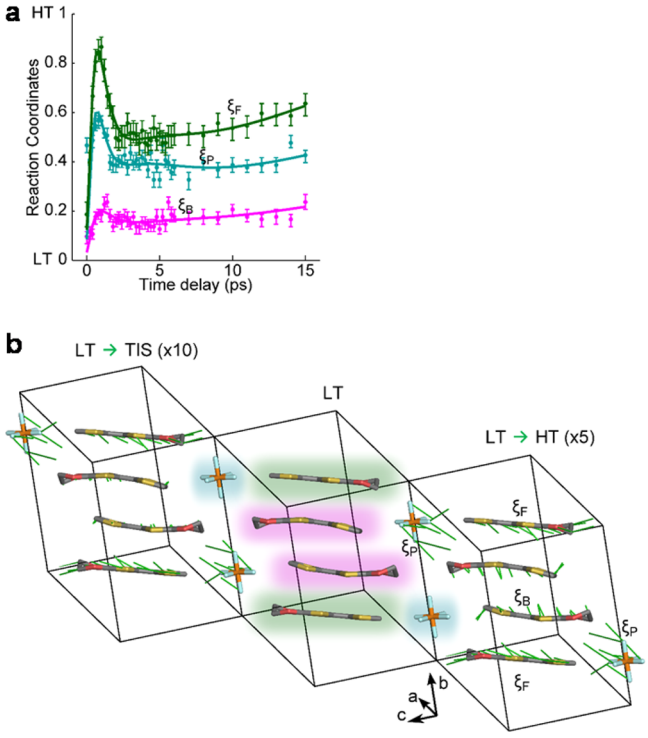

Figure 12. (a) Temporal variations of the reaction coordinates ξ_F, ξ_B, and ξ_P. (b) Crystal structure of $(EDO\text{-}TTF)_2PF_6$ before photoexcitation (middle) and displacements of atoms (represented by green lines) in the phase transition from 230 K (LT) to 295 K (HT) (right) and in the photoinduced phase transition (TIS) at 3−10 ps after photoexcitation (left). Adapted with permission from ref 45. Copyright 2013 Nature Publishing Group.

(TIS) at 3−10 ps after photoexcitation and the high-temperature phase, respectively.

Intriguingly, the structural period in the TIS consists of four EDO-TTF molecules even though the flat monovalent molecules undergo translations; in contrast, the optical measurements implied that the period of charge distribution involved two EDO-TTFs to obtain the (0, 1, 0, 1) charge ordering. This indicates that in this time region, the lattice and electronic structures differ. The unmovable EDO-TTF that is bent as a result of steric interactions presumably plays an important role in creating the unique photoinduced phase. This speculation is consistent with the fact that coherent intramolecular vibrations at 1300 cm^{-1} are strongly involved in the emergence of the photoinduced phase described in section 3. Furthermore, the large movement of the PF_6 counteranion from the beginning is consistent with the theoretical calculation that anion displacement plays an important role in the emergence of the photoinduced phase.[19] This behavior is also in good agreement with previous results in which slow structural changes were observed in other CT complexes having steric hindrance.[17] The experimental fact that the flat EDO-TTF slips away from the bent EDO-TTF explains the observation of 66 cm^{-1} coherent oscillations, which correspond to intermolecular vibrations. The importance of the counteranion in photoexcited dynamics has also been reported in another type of ionic crystal on the basis of femtosecond X-ray diffraction.[46]

7. CONCLUDING REMARKS

Diverse photoinduced dynamics in $(EDO\text{-}TTF)_2PF_6$, an organic crystal that has strong electron−electron and electron−phonon interactions, have been studied by a combination of various ultrafast measurement techniques, including electronic spectroscopy on 10 and 100 fs time scales, infrared vibrational spectroscopy, and electron diffraction. After photoexcitation of the charge-localized low-temperature phase, a photoinduced phase having a new charge order emerges over 40 fs; this new phase has never been observed in the crystal at thermal equilibrium. Subsequently, over ∼100 ps, the charge-ordered phase melts and a phase similar to the metallic high-temperature phase emerges. In these phase transitions, the steric effects of the bent EDO-TTF and the motions of flat EDO-TTF and PF_6 play important roles.

Recently it has been determined that various states emerge and vanish in nonequilibrium states of strongly correlated materials such as $(EDO\text{-}TTF)_2PF_6$. When these dynamics are well-understood and appropriately used, various physical properties such as electrical conductivity and magnetism can be controlled on time scales that have never been achieved by conventional methods. In these types of materials, even mechanical movements could be controlled via strong electron−lattice interactions. In terms of photoenergy conversion, fast and efficient energy transfer could be achieved using cooperative phenomena in strongly correlated materials. However, studies of nonequilibrium states in strongly correlated materials are very difficult both experimentally and theoretically; thus, novel ultrafast measurement techniques and theories need to be developed to overcome these difficulties.

AUTHOR INFORMATION

Corresponding Author

*E-mail: onda.k.aa@m.titecha.jp.

Notes

The authors declare no competing financial interest.

Biographies

Ken Onda is a researcher of PRESTO of the Japan Science and Technology Agency and has worked at Tokyo Institute of Technology since 2013. His main research interests are studying the chemical reaction dynamics of complex functional materials using various ultrafast measurement techniques.

Hideki Yamochi is a Professor at the Research Center for Low Temperature and Materials Sciences at Kyoto University. He develops functional organic materials concerning itinerant electrons.

Shin-ya Koshihara has been a Professor at the Department of Chemistry and Materials Science at Tokyo Institute of Technology since 2000. His research has mainly been devoted to photocontrol of cooperative phenomena (photoinduced phase transitions). His research includes utilizing ultrafast spectroscopic measurements and expanding the research field into dynamical structures based on pulsed X-rays and electrons.

ACKNOWLEDGMENTS

The authors acknowledge Professor Yoichi Okimoto, Dr. Tadahiko Ishikawa (Tokyo Institute of Technology), Professor Kenji Yonemitsu (Chuo University), Professor Gunzi Saito (Meijo University), Professor Xiangfeng Shao (Lanzhou University), Dr. Yoshiaki Nakano (Kyoto University), Professor Germán Sciaini (University of Waterloo), and Professor R. J.

Dwayne Miller (University of Toronto, University of Hamburg) for their support and contributions to this study.

REFERENCES

(1) Kagoshima, S., Kanoda, K., Mori, T., Eds. Special Topics on Organic Conductors. *J. Phys. Soc. Jpn.* **2006**, *75*, Nos. 051001−051016.

(2) Saito, G.; Yoshida, Y. Development of conductive organic molecular assemblies: Organic metals, superconductors, and exotic functional materials. *Bull. Chem. Soc. Jpn.* **2007**, *80*, 1−137.

(3) Uji, S., Mori. T., Takahashi, T., Eds. Topical Review on Focus on Organic Conductors. *Sci. Technol. Adv. Mater.* **2009**, *10*, 020301−025005.

(4) Brooks, J. S. Organic crystals: Properties, devices, functionalization and bridges to bio-molecules. *Chem. Soc. Rev.* **2010**, *39*, 2667−2694.

(5) Mori, T. Structural genealogy of BEDT-TTF-based organic conductors I. Parallel molecules: *b* and *b″* phases. *Bull. Chem. Soc. Jpn.* **1998**, *71*, 2509−2526.

(6) Mori, T. Structural genealogy of BEDT-TTF-based organic conductors II. Inclined molecules: *q*, *a*, and *c* phases. *Bull. Chem. Soc. Jpn.* **1999**, *72*, 179−197.

(7) Seo, H.; Hotta, C.; Fukuyama, H. Toward systematic understanding of diversity of electronic properties in low-dimensional molecular solids. *Chem. Rev.* **2004**, *104*, 5005−5036.

(8) Koshihara, S.; Tokura, Y.; Mitani, T.; Saito, G.; Koda, T. Photoinduced valence instability in the organic molecular compound tetrathiafulvalene-*p*-chloranil (TTF-CA). *Phys. Rev. B* **1990**, *44*, 6853−6856.

(9) Iwai, S.; Tanaka, S.; Fujinuma, K.; Kishida, H.; Okamoto, H.; Tokura, Y. Ultrafast optical switching from an ionic to a neutral state in tetrathiafulvalene-*p*-chloranil (TTF-CA) observed in femtosecond reflection spectroscopy. *Phys. Rev. Lett.* **2002**, *88*, No. 057402.

(10) Tanimura, K. Femtosecond time-resolved reflection spectroscopy of photoinduced ionic−neutral phase transition in TTF-CA crystals. *Phys. Rev. B* **2004**, *70*, No. 144112.

(11) Okamato, H.; Ishige, Y.; Tanaka, S.; Kishida, H.; Iwai, S.; Tokura, Y. Photoinduced phase transition in tetrathiafulvalene-*p*-chloranil observed in femtosecond reflection spectroscopy. *Phys. Rev. B* **2004**, *70*, No. 165202.

(12) Okamoto, H.; Ikegami, K.; Wakabayashi, T.; Ishige, Y.; Togo, J.; Kishida, H.; Matsuzaki, H. Ultrafast photoinduced melting of a spin-Peierls phase in an organic charge-transfer compound, K-tetracyanoquinodimethane. *Phys. Rev. Lett.* **2006**, *96*, No. 037405.

(13) Uemura, H.; Matsuzaki, H.; Takahashi, Y.; Hasegawa, T.; Okamoto, H. Ultrafast charge dynamics in one-dimensional organic Mott insulators. *J. Phys. Soc. Jpn.* **2008**, *77*, No. 113714.

(14) Iwai, S.; Yamamoto, K.; Kashiwazaki, A.; Hiramatsu, F.; Nakaya, H.; Kawakami, Y.; Yakushi, K.; Okamoto, H.; Mori, H.; Nishio, Y. Photoinduced melting of a stripe-type charge-order and metallic domain formation in a layered BEDT-TTF-based organic salt. *Phys. Rev. Lett.* **2007**, *98*, No. 097402.

(15) Kawakami, K.; Iwai, S.; Fukatsu, T.; Miura, M.; Yoneyama, N.; Sasaki, T.; Kobayashi, N. Optical modulation of effective on-site Coulomb energy for the Mott transition in an organic dimer insulator. *Phys. Rev. Lett.* **2009**, *103*, No. 066403.

(16) Ishikawa, T.; Fukazawa, N.; Matsubara, Y.; Nakajima, R.; Onda, K.; Okimoto, Y.; Koshihara, S.; Lorenc, M.; Collet, E.; Tamura, M.; Kato, R. Large and ultrafast photoinduced reflectivity change in the charge separated phase of $Et_2Me_2Sb[Pd(1,3\text{-dithiol-2-thione-4,5-dithiolate})_2]_2$. *Phys. Rev. B* **2009**, *80*, No. 115108.

(17) Fukazawa, N.; Tanaka, T.; Ishikawa, T.; Okimoto, Y.; Koshihara, S.; Yamamoto, T.; Tamura, M.; Kato, R.; Onda, K. Time-resolved infrared vibrational spectroscopy of the photoinduced phase transition of $Pd(dmit)_2$ salts having different orders of phase transition. *J. Phys. Chem. C* **2013**, *117*, 13187−13196.

(18) Chollet, M.; Guerin, L.; Uchida, N.; Fukaya, S.; Shimoda, H.; Ishikawa, T.; Matsuda, K.; Hasegawa, T.; Ota, A.; Yamochi, H.; Saito, G.; Tazaki, R.; Adachi, S.; Koshihara, S. Gigantic photoresponse in 1/4-filled-band organic salt $(EDO\text{-}TTF)_2PF_6$. *Science* **2005**, *307*, 86−89.

(19) Onda, K.; Ogihara, S.; Yonemitsu, K.; Maeshima, N.; Ishikawa, T.; Okimoto, Y.; Shao, X. F.; Nakano, Y.; Yamochi, H.; Saito, G.; Koshihara, S. Photoinduced change in the charge order pattern in the quarter-filled organic conductor $(EDO\text{-}TTF)_2PF_6$ with a strong electron−phonon interaction. *Phys. Rev. Lett.* **2008**, *101*, No. 067403.

(20) Ota, A.; Yamochi, H.; Saito, G. A novel metal−insulator phase transition observed in $(EDO\text{-}TTF)_2PF_6$. *J. Mater. Chem.* **2002**, *12*, 2600−2602.

(21) Ota, A.; Yamochi, H.; Saito, G. A novel metal−insulator transition in $(EDO\text{-}TTF)_2X$ (X = PF_6 and AsF_6). *Synth. Met.* **2003**, *133−134*, 463−465.

(22) Aoyagi, S.; Kato, K.; Ota, A.; Yamochi, H.; Saito, G.; Suematsu, H.; Sakata, M.; Takata, M. Direct observation of bonding and charge ordering in $(EDO\text{-}TTF)_2PF_6$. *Angew. Chem., Int. Ed.* **2004**, *43*, 3670−3673.

(23) Drozdova, O.; Yakushi, K.; Ota, A.; Yamochi, H.; Saito, G. Spectroscopic study of the [0110] charge ordering in $(EDO\text{-}TTF)_2PF_6$. *Synth. Met.* **2003**, *133−134*, 277−279.

(24) Drozdova, O.; Yakushi, K.; Yamamoto, K.; Ota, A.; Yamochi, H.; Saito, G.; Tashiro, H.; Tanner, D. B. Optical characterization of $2k_F$ bond-charge-density wave in quasi-one-dimensional 3/4-filled $(EDO\text{-}TTF)_2X$ (X = PF_6 and AsF_6). *Phys. Rev. B* **2004**, *70*, No. 075107.

(25) Matsubara, Y.; Ogihara, S.; Itatani, J.; Maeshima, N.; Yonemitsu, K.; Ishikawa, T.; Okimoto, Y.; Koshihara, S.; Hiramatsu, T.; Nakano, Y.; Yamochi, H.; Saito, G.; Onda, K. Coherent dynamics of photoinduced phase formation in a strongly correlated organic crystal. *Phys. Rev. B* **2014**, *89*, No. 161102.

(26) Brist Cruz, C. H.; Gordon, J. P.; Becker, P. C.; Fork, R. L.; Shank, C. V. Dynamics of spectral hole burning. *IEEE J. Quantum Electron.* **1988**, *24*, 261−266.

(27) Pollard, W. T.; Dexheimer, S. L.; Wang, Q.; Peteeanu, L. A.; Shank, C. V.; Mathies, R. A. Theory of dynamic absorption spectroscopy of nonstationary states. 4. Application to 12-fs resonant impulsive Raman spectroscopy of bacteriorhodopsin. *J. Phys. Chem.* **1992**, *96*, 6147−6158.

(28) Hamm, P. Coherent effects in femtosecond infrared spectroscopy. *Chem. Phys.* **1995**, *200*, 415−429.

(29) Kobayashi, T.; Du, J.; Feng, W.; Yoshino, K. Excited-state molecular vibration observed for a probe pulse preceding the pump pulse by real-time optical spectroscopy. *Phys. Rev. Lett.* **2008**, *101*, No. 037402.

(30) Kawakami, Y.; Fukatsu, T.; Sakurai, Y.; Unno, H.; Itoh, H.; Iwai, S.; Sasaki, T.; Yamamoto, K.; Yakushi, K.; Yonemitsu, K. Early-Stage Dynamics of Light−Matter Interaction Leading to the Insulator-to-Metal Transition in a Charge Ordered Organic Crystal. *Phys. Rev. Lett.* **2010**, *105*, No. 246402.

(31) Nasu, K. *Photo-Induced Phase Transition*; World Scientific: Singapore, 2003.

(32) Gonokami, M., Koshihara, S., Eds.; Special Issue on Photo-Induced Phase Transitions and Their Dynamics *J. Phys. Soc. Jpn.* **2006**, *75*, Nos. 011001−011008.

(33) Onda, K.; Ogihara, S.; Ishikawa, T.; Okimoto, Y.; Shao, X. F.; Yamochi, H.; Saito, G.; Koshihara, S. The photo-induced phase and coherent phonon in the organic conductor $(EDO\text{-}TTF)_2PF_6$. *J. Phys.: Condens. Matter* **2008**, *20*, No. 224018.

(34) Yonemitsu, K.; Maeshima, N. Photoinduced melting of charge order in a quarter-filled electron system coupled with different types of phonons. *Phys. Rev. B* **2007**, *76*, No. 075105.

(35) Fukazawa, N.; Shimizu, M.; Ishikawa, T.; Okimoto, Y.; Koshihara, S.; Hiramatsu, T.; Nakano, Y.; Yamochi, H.; Saito, G.; Onda, K. Charge and structural dynamics in photoinduced phase transition of $(EDO\text{-}TTF)_2PF_6$ examined by picosecond time-resolved vibrational spectroscopy. *J. Phys. Chem. C* **2012**, *116*, 5892−5899.

(36) Matsubara, Y.; Okimoto, Y.; Yoshida, T.; Ishikawa, T.; Koshihara, S.; Onda, K. Photoinduced neutral-to-ionic phase transition in tetrathiafulvalene-*p*-chloranil studied by time-resolved vibrational spectroscopy. *J. Phys. Soc. Jpn.* **2011**, *80*, No. 124711.

(37) Matsubara, Y.; Yoshida, T.; Ishikawa, T.; Okimoto, Y.; Koshihara, S.; Onda, K. Photoinduced ionic to neutral phase transition

in TTF-CA studied by time-resolved infrared vibrational spectroscopy. *Acta Phys. Pol., A* **2012**, *121*, 340−342.
(38) Yamamoto, T.; Uruichi, M.; Yamamoto, K.; Yakushi, K.; Kawamoto, A.; Taniguchi, H. Examination of the charge-sensitive vibrational modes in bis(ethylenedithio)tetrathiafulvalene. *J. Phys. Chem. B* **2005**, *109*, 15226−15235.
(39) Yamamoto, T.; Nakazawa, Y.; Tamura, M.; Fukunaga, T.; Kato, R.; Yakushi, K. Vibrational spectra of $[Pd(dmit)_2]$ dimer (dmit = 1,3-dithiole-2-thione-4,5-dithiolate): Methodology for examining charge, inter-molecular interactions, and orbital. *J. Phys. Soc. Jpn.* **2011**, *80*, No. 074717.
(40) Siwick, B. J.; Green, A. A.; Hebeisen, C. T.; Miller, R. J. D. Characterization of ultrashort electron pulses by electron−laser pulse cross correlation. *Opt. Lett.* **2005**, *30*, 1057−1059.
(41) Gao, M.; Jean-Ruel, H.; Cooney, R. R.; Stampe, J.; de Jong, M.; Harb, M.; Sciaini, G.; Moriena, G.; Miller, R. J. D. Full characterization of RF compressed femtosecond electron pulses using ponderomotive scattering. *Opt. Express* **2012**, *20*, 12048−12058.
(42) van Oudheusden, T.; Pasmans, P. L. E. M.; van der Geer, S. B.; de Loos, M. J.; van der Wiel, M. J.; Luiten, O. J. Compression of subrelativistic space-charge-dominated electron bunches for single-shot femtosecond electron diffraction. *Phys. Rev. Lett.* **2010**, *105*, No. 264801.
(43) Gahlmann, A.; Park, S. T.; Zewail, A. H. Ultrashort electron pulses for diffraction, crystallography and microscopy: Theoretical and experimental resolutions. *Phys. Chem. Chem. Phys.* **2008**, *10*, 2894−2909.
(44) Aidelsburger, M.; Kirchner, F. O.; Krausz, F.; Baum, P. Single-electron pulses for ultrafast diffraction. *Proc. Natl. Acad. Sci. U.S.A.* **2010**, *107*, 19714−19719.
(45) Gao, M.; Lu, C.; Jean-Ruel, H.; Liu, L. C.; Marx, A.; Onda, K.; Koshihara, S.; Nakano, Y.; Shao, X. F.; Hiramatsu, T.; Saito, G.; Yamochi, H.; Cooney, R. R.; Moriena, G.; Sciaini, G.; Miller, R. J. D. Mapping molecular motions leading to charge delocalization with ultrabright electrons. *Nature* **2013**, *496*, 343−346.
(46) Freyer, B.; Zamponi, F.; Juvé, V.; Stingl, J.; Woerner, M.; Elsaesser, T.; Chergui, M. Ultrafast inter-ionic charge transfer of transition-metal complexes mapped by femtosecond X-ray powder diffraction. *J. Chem. Phys.* **2013**, *138*, No. 144504.